

Mixed-Precision Embeddings for Large-Scale Recommendation Models

Shiwei Li*

Huazhong University of Science and
Technology
Wuhan, China
lishiwei@hust.edu.cn

Zhuoqi Hu

Huazhong University of Science and
Technology
Wuhan, China
qzhycloud@outlook.com

Xing Tang

FiT, Tencent
Shenzhen, China
xing.tang@hotmail.com

Haozhao Wang

Huazhong University of Science and
Technology
Wuhan, China
hz_wang@hust.edu.cn

Shijie Xu

FiT, Tencent
Shenzhen, China
shijiexu@tencent.com

Weihong Luo

FiT, Tencent
Shenzhen, China
lobbyluo@tencent.com

Yuhua Li

Huazhong University of Science and
Technology
Wuhan, China
idcliyuhua@hust.edu.cn

Xiuqiang He

FiT, Tencent
Shenzhen, China
xiuqianghe@tencent.com

Ruixuan Li†

Huazhong University of Science and
Technology
Wuhan, China
rxli@hust.edu.cn

ABSTRACT

Embedding techniques have become essential components of large databases in the deep learning era. By encoding discrete entities, such as words, items, or graph nodes, into continuous vector spaces, embeddings facilitate more efficient storage, retrieval, and processing in large databases. Especially in the domain of recommender systems, millions of categorical features are encoded as unique embedding vectors, which facilitates the modeling of similarities and interactions among features. However, numerous embedding vectors can result in significant storage overhead. In this paper, we aim to compress the embedding table through quantization techniques. Given that features vary in importance levels, we seek to identify an appropriate precision for each feature to balance model accuracy and memory usage. To this end, we propose a novel embedding compression method, termed Mixed-Precision Embeddings (MPE). Specifically, to reduce the size of the search space, we first group features by frequency and then search precision for each feature group. MPE further learns the probability distribution over precision levels for each feature group, which can be used to identify the most suitable precision with a specially designed sampling strategy. Extensive experiments on three public datasets demonstrate that MPE significantly outperforms existing embedding compression methods. Remarkably, MPE achieves about 200x compression on the Criteo dataset without comprising the prediction accuracy.

PVLDB Reference Format:

Shiwei Li, Zhuoqi Hu, Xing Tang, Haozhao Wang, Shijie Xu, Weihong Luo, Yuhua Li, Xiuqiang He, and Ruixuan Li. Mixed-Precision Embeddings for Large-Scale Recommendation Models. PVLDB, 14(1): XXX-XXX, 2020.

doi:XX.XX/XXX.XX

*This work was done when Shiwei Li worked as an intern at FiT, Tencent.

†Ruixuan Li is the corresponding author.

This work is licensed under the Creative Commons BY-NC-ND 4.0 International License. Visit <https://creativecommons.org/licenses/by-nc-nd/4.0/> to view a copy of

PVLDB Artifact Availability:

The source code, data, and/or other artifacts have been made available at <https://github.com/Leopold1423/mpe>.

1 INTRODUCTION

1.1 Background

In the deep learning era, embedding techniques have become essential components of large databases due to their effectiveness and efficiency in representing and retrieving information [14, 32]. By encoding discrete entities, such as words, items, or graph nodes, into continuous vector spaces, embeddings facilitate more efficient storage, retrieval, and processing within large databases. These techniques are now widely applied across various domains, including natural language processing [36, 41], graph learning [12, 26], and recommender systems [28, 60, 66]. In particular, embedding techniques have a great impact on recommender systems, where the number of required embeddings far exceeds that of other domains. Specifically, the input data in recommender systems typically consists of various attributes, such as user_id, age, and occupation, each with multiple possible values. These attributes are often referred to as feature fields, while their specific values are known as categorical features or simply features. Each categorical feature will be represented by a unique embedding vector, which enhances the modeling of similarities and interactions among features, thereby improving the accuracy of recommendations. However, the amount of categorical features in recommender systems is significantly larger than that of discrete entities in other domains. For example,

this license. For any use beyond those covered by this license, obtain permission by emailing info@vldb.org. Copyright is held by the owner/author(s). Publication rights licensed to the VLDB Endowment.

Proceedings of the VLDB Endowment, Vol. 14, No. 1 ISSN 2150-8097.

doi:XX.XX/XXX.XX

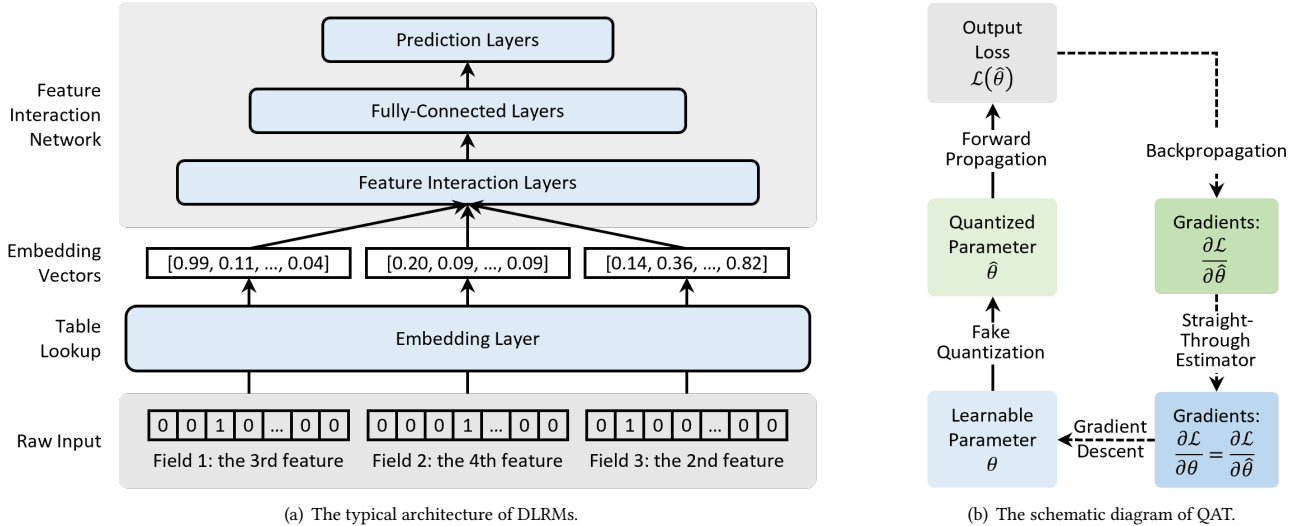


Figure 1: The typical architecture of deep learning recommendation models (DLRMs) and the schematic diagram of quantization-aware training (QAT). (a) DLRMs are usually composed of an embedding layer and a feature interaction network. (b) A fake quantizer will be inserted into the forward propagation of QAT, and end-to-end optimization is then achieved through Straight-Through Estimator (STE), which treats the quantizer as an identity map during backpropagation.

an ordinary advertising system in Baidu contains billions of features [58]. In contrast, the vocabulary size of the large language model LLaMA 3 [8] is only 128,000, with the former being several orders of magnitude larger. Therefore, embedding techniques are particularly important in recommender systems.

The embedding techniques are commonly adopted as part of the deep learning recommendation models (DLRMs). The typical architecture of DLRMs includes an embedding table that converts categorical features into dense vector representations, followed by a feature interaction network that processes these embeddings to generate predictions, as illustrated in Figure 1(a). Numerous studies have refined the structure of the feature interaction network to improve prediction accuracy [15, 33, 42, 51, 52, 56]. Despite these improvements, the interaction networks often have relatively shallow layers and a limited number of parameters, while the majority of model parameters are concentrated in the embedding table. Especially when handling billions of categorical features, the storage of the embedding table can even reach 10 TB [58]. Therefore, developing techniques to compress embeddings while maintaining model accuracy has become a crucial issue in deploying DLRMs.

Regarding model compression, quantization is undoubtedly one of the most effective techniques [38], which reduces memory usage by representing parameters with fewer bits. There are two primary methods of quantization: post-training quantization (PTQ) [13, 37] and quantization-aware training (QAT) [2, 9, 39]. PTQ applies quantization after the training process, while QAT incorporates a quantization operator during training. As shown in Figure 1(b), QAT inserts a fake quantization operator into the forward propagation, allowing the model to better adapt to quantization and thus achieve higher accuracy than PTQ. During backpropagation, the learnable parameters are updated using the Straight-Through Estimator (STE)

[17], approximating the gradient of the non-differentiable quantization operator as 1, thereby enabling end-to-end optimization. After training, the parameters will be quantized and then stored in a low-precision format for deployment.

1.2 Motivation and Contributions

An embedding table can be represented by a matrix $E \in \mathbb{R}^{n \times d}$, where n is the number of categorical features, and d is the dimension of each embedding vector. As discussed by Zhang et al. [65], existing methods generally compress either the rows or columns of the embedding table. Row compression methods involve techniques like feature selection [16, 22, 25, 34] and hashing [45, 59, 64, 65]. For example, OptFS [34] filters out unimportant features to reduce the number of rows in the embedding table, while Zhang et al. [64] propose sharing embeddings among infrequent features through hash functions, thereby reusing rows. On the other hand, dimension compression methods involve techniques like mixed-dimension embeddings [35, 47, 67, 68] and pruning [6, 31, 57]. For example, CpRec [47] assigns varying dimensions to embeddings of different features, while PEP [31] prunes redundant parameters within each feature embedding by learning a threshold. A key characteristic of these methods is their ability to explicitly or implicitly assess feature importance and allocate storage space accordingly.

In addition to row and column perspectives, parameter precision is another critical perspective of embedding compression, closely related to quantization techniques. Guan et al. [13] were the first to apply PTQ to embedding tables. Later studies [27, 58, 61] have focused on the low-precision training (LPT) paradigm. Unlike QAT, which retains full-precision parameters during training, LPT keeps embeddings in a low-precision format throughout training to reduce training memory usage. However, at lower precision levels,

LPT becomes impractical due to significant accuracy loss. For example, ALPT [27] achieves lossless compression only at 8-bit precision. Note that recommender systems typically cannot tolerate any degradation in accuracy. Beyond these efforts, there has been little in-depth research on quantization, particularly QAT, within recommender systems. This scarcity is largely attributable to the unique characteristic of embedding tables in recommender systems, which render quantization techniques less prevalent compared to domains such as computer vision [9] and natural language processing [18]. Specifically, embedding tables often contain many features with varying levels of importance. Yet, quantization typically applies uniform precision across all embeddings, failing to distinguish feature importance. As a result, numerous less important features are assigned the same precision as more significant ones, even though they could be represented with lower precision, leading to inefficient compression.

In this paper, we aim to improve the quantization of embedding tables by incorporating the ability to distinguish feature importance. Previous studies have linked feature importance to the embedding dimension [47], the utilization of the feature [34] and so on. Similarly, we propose to associate feature importance with embedding precision. More precisely, our objective is to find the most appropriate precision for each feature embedding to balance model accuracy with memory efficiency. It is worth noting that feature selection can be viewed as a binary case of mixed-precision embeddings, where the search space includes only zero-precision and full-precision options. Therefore, mixed-precision embeddings can achieve finer-grained compression than feature selection methods.

To solve the problem of searching embedding precision, we propose a novel algorithm named Mixed-Precision Embeddings (MPE). There are two main challenges in building MPE. The first challenge is the vast number of categorical features. DLRMs typically involve millions of categorical features, resulting in an excessively large search space when searching precision for each feature individually. To mitigate this issue, we propose grouping features and optimizing precision for each group, substantially reducing search space complexity. Previous research has identified feature frequency as a reliable measure of feature importance [25, 64]. Therefore, we suggest grouping features by frequency to ensure that features within the same group have similar levels of importance, thereby minimizing conflicts from shared precision. The second challenge is determining each feature group’s precision (i.e., quantization bit-width). However, precision search is inherently a discrete problem that traditional gradient descent algorithms cannot solve effectively. To achieve end-to-end optimization, we propose learning a probability distribution over candidate bit-widths for each group, where output embeddings will be represented as the expected values of quantized embeddings across all candidate bit-widths. Additionally, we apply regularization to the expected bit-width of groups to minimize memory usage. By balancing the objective function with this regularization, we can effectively learn the optimal probability distribution over candidate bit-widths. Finally, we sample the precision based on the optimized probability distribution and then retrain the model to enhance accuracy.

Our main contributions can be summarized as follows:

- We identify a critical limitation of quantization-aware training in embedding compression for recommendation models, namely, its inability to distinguish feature importance.
- We propose a novel embedding compression method, MPE, that can implicitly distinguish feature importance. Specifically, MPE identifies an appropriate precision for each feature embedding.
- We evaluate MPE on three large-scale public datasets across various models. The experimental results demonstrate MPE significantly outperforms existing embedding compression methods.

2 PRELIMINARIES

In this section, we provide a formal definition of deep learning recommendation models and quantization-aware training.

2.1 Deep Learning Recommendation Models

Figure 1(a) illustrates the general architecture of DLRMs, which includes an embedding layer \mathcal{E} and a feature interaction network \mathcal{F} . For simplicity, we use E and W to denote the parameters within the embedding layer and the feature interaction network, respectively. The embedding layer maps categorical features x into dense embeddings, represented as $\mathcal{E}(x) = \mathcal{I}(x)^T E$, where x is the input features and $\mathcal{I}(x)$ is the corresponding one-hot encoded vectors as shown in Figure 1(a). These embeddings are then processed by the following network to generate predictions. Denoting the dataset by \mathbb{D} and the loss function by \mathcal{L} , the optimization process of DLRMs can be formulated as follows:

$$\min_{E, W} \sum_{(x, y) \in \mathbb{D}} \mathcal{L}(y, \mathcal{F}(\mathcal{E}(x, E), W)) \quad (1)$$

The commonly used notations are summarized in Table 1.

Table 1: Commonly used notations and descriptions.

Notation	Description
\mathbb{D}	Dataset.
\mathcal{L}	Loss function.
\mathcal{E}	Function of the embedding layer.
\mathcal{F}	Function of the feature interaction network.
E	Parameters within the embedding table.
W	Parameters within the feature interaction network.
n, d	Number of features and embedding dimension.
x, y	Input features x and the label y of a data sample.
Q	Quantizer.
\mathbb{B}	Set of candidate bit-widths.
m	Number of candidate bit-widths.
b, α, β	Bit-width, step size, and offset of quantization.
N_b, P_b	Negative and positive bounds of b -bit signed integers.
e, \hat{e}	Full-precision and quantized embedding vector.
g	Number of feature groups.
s^k	Sum of the feature frequencies in the k -th group.
γ	Learnable probability distribution parameters.
τ	Temperature coefficient in the softmax function.
p	Probability distribution over precision levels.
λ	Regularization coefficient of expected bit-width.

2.2 Quantization-Aware Training

In the context of neural networks, quantization is to reduce the precision of parameters. By converting full-precision weights into lower-precision formats, such as 8-bit integers, quantization can significantly decrease the memory usage of neural networks. Consequently, we seek to reduce the storage overhead of embedding tables through quantization. It is worth noting that we do not quantize the feature interaction network, as doing so would severely hurt prediction accuracy while yielding little memory savings.

In this paper, we employ the uniform quantization [38] to compress embedding tables. Specifically, given a step size α , an offset β , and the quantization bit-width b , a full-precision number θ will be quantized as follows:

$$\begin{aligned}\hat{\theta} &= Q(\theta, \alpha, \beta, b) = \alpha\bar{\theta} + \beta, \\ \bar{\theta} &= \text{clamp}(\lfloor \frac{\theta - \beta}{\alpha} \rfloor, N_b, P_b), \\ N_b &= -2^{m-1}, \quad P_b = 2^{m-1} - 1,\end{aligned}\quad (2)$$

where $\hat{\theta}$ and $\bar{\theta}$ are the quantized value and corresponding integer value, respectively. N_b and P_b are the negative and positive bounds of a b -bit signed integer, respectively. $\lfloor x \rfloor$ rounds x to its nearest integer and the function $\text{clamp}(\cdot)$ ensures that the returned integer stays within $[N_b, P_b]$. The step size α determines the granularity of the quantization, and the offset β is the center of the quantized values. Note that α and β are shared across lots of parameters, such as those within each layer, making their storage negligible. As illustrated in Figure 1(b), the above quantizer Q can be inserted into a network to facilitate QAT. When applying b -bit QAT to embedding tables, the training objective of DLRMs can be formulated as follows:

$$\min_{E, \alpha, \beta, W} \sum_{(x, y) \in \mathbb{D}} \mathcal{L}(y, \mathcal{F}(\mathcal{E}(x, Q(E, \alpha, \beta, b)), W)) \quad (3)$$

However, the non-differentiable nature of the quantizer Q , particularly due to the rounding function, presents challenges for optimization with gradient descent algorithms. Previous work has utilized the Straight-through Estimator (STE) [17] to approximate the gradient of the quantizer as 1. In this paper, we employ an advanced QAT algorithm, LSQ+ [2], as the base quantizer, which similarly approximates the gradient of the rounding function as 1. This allows the gradients for the input parameters θ , α , and β to be calculated, as detailed below:

$$\frac{\partial \hat{\theta}}{\partial \theta} = \frac{\partial \bar{\theta}}{\partial \theta} \alpha = \begin{cases} 1 & \text{if } N_b < \frac{\theta - \beta}{\alpha} < P_b, \\ 0 & \text{otherwise.} \end{cases} \quad (4)$$

$$\frac{\partial \hat{\theta}}{\partial \alpha} = \frac{\partial \bar{\theta}}{\partial \alpha} \alpha + \bar{\theta} = \begin{cases} N_b & \text{if } \frac{\theta - \beta}{\alpha} \leq N_b, \\ -\frac{\theta - \beta}{\alpha} + \lfloor \frac{\theta - \beta}{\alpha} \rfloor & \text{if } N_b < \frac{\theta - \beta}{\alpha} < P_b, \\ P_b & \text{if } \frac{\theta - \beta}{\alpha} \geq P_b. \end{cases} \quad (5)$$

$$\frac{\partial \hat{\theta}}{\partial \beta} = \frac{\partial \bar{\theta}}{\partial \beta} \alpha + 1 = \begin{cases} 0 & \text{if } N_b < \frac{\theta - \beta}{\alpha} < P_b \\ 1 & \text{otherwise.} \end{cases} \quad (6)$$

3 MIXED-PRECISION EMBEDDINGS

In this section, we first provide a formal definition of embedding precision search problem in Section 3.1. Then, we introduce how to

reduce the complexity of the search space in Section 3.2 and how to search precision for feature embedding in Section 3.3. Finally, we illustrate how to generate mixed-precision embedding with the searched precision in Section 3.4.

3.1 Problem Formulation

It is a consensus that categorical features in recommender systems have varying levels of importance [34, 64]. Previous studies leveraged this variation in feature importance to reduce the parameters associated with less important features [25, 34, 64, 67]. For example, Sun et al. [47] reduces the embedding dimension of less important features through heuristic rules, while AutoEmb [67] automatically searches embedding dimensions with reinforcement learning algorithms. Additionally, AdaEmbed [25] uses gradient information and feature frequencies to access feature importance and then prunes unimportant features. Despite these advancements, no prior work has systematically combined feature importance with corresponding embedding precision. In this paper, to achieve more efficient embedding compression, we propose searching for an optimal precision level for each feature, which refers to the smallest bit-width without losing prediction accuracy.

Given a set of candidate precision levels (i.e., bit-widths), $\mathbb{B} = \{b_1, b_2, \dots, b_m\}$, we aim to determine $B \in \mathbb{B}^{n \times 1}$ for the embedding table $E \in \mathbb{R}^{n \times d}$, where each element of B represents the precision of the corresponding embedding in E . Specifically, the problem of mixed-precision embedding can be formally defined as follows:

$$\begin{aligned}\min_{B, E, \alpha, \beta, W} \quad & \sum_{(x, y) \in \mathbb{D}} \mathcal{L}(y, \mathcal{F}(\mathcal{E}(x, Q(E, \alpha, \beta, B)), W)), \\ \text{s.t.} \quad & \|B\|_1 \leq n \times B^*,\end{aligned}\quad (7)$$

where B^* is the average bit-width budget and B is included as a parameter of Q to signify mixed-precision quantization. Notably, the step size α and the offset β are still shared across numerous parameters. Additionally, when 0 is included in \mathbb{B} and assigned to a feature, the corresponding embedding is set to a zero vector. In this case, it also serves as a feature selection mechanism.

3.2 Frequency-Aware Grouping

Due to the large number of features, the search space for embedding precision becomes vast, complicating the optimization of Eq.(7). However, since the number of candidate bit-widths is significantly smaller than the number of features, many features can share the same bit-width. Therefore, we can group features in advance and ensure that features in the same group can satisfy the same bit-width. Feature frequency, a common measure of feature importance used in numerous studies [23, 25, 47, 64], is employed here as prior information to guide the grouping process. Specifically, features are sorted by frequency and divided into g groups, with a bit-width searched for each group individually. This simple strategy reduces the search space complexity by a factor of n/g while minimizing conflicts arising from the shared bit-width within a group.

3.3 Learnable Probability Distribution

In the previous section, we reduced the search space by grouping features. The remaining challenge is determining the optimal precision for each feature group. However, optimizing the embedding

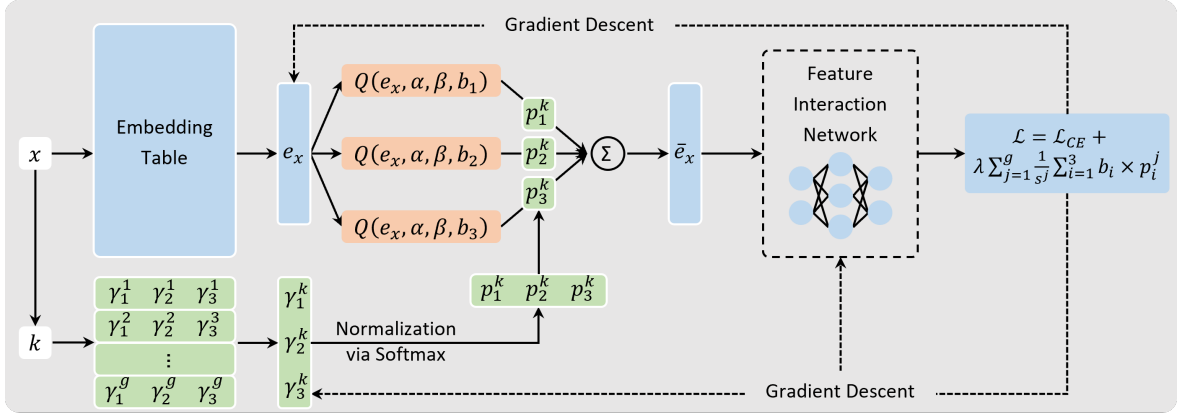


Figure 2: Learning process of the probability distribution over candidate bit-widths in MPE. x is a feature of the input data, and k is the corresponding group index when sorted by feature frequency.

precision is more complex than solving discrete problems like feature selection or embedding dimension search. Feature selection is a simple decision about whether to include a feature while embedding dimension search involves selecting from multiple candidate dimensions. In contrast, mixed-precision embedding presents two discrete optimization problems: selecting from multiple candidate bit-widths and managing non-differentiable quantization operators.

Inspired by traditional QAT algorithms, we employ the STE to handle the non-differentiability of quantization operators. Further, to optimize the precision of different feature groups in an end-to-end manner, we convert the one-hot selection of candidate bit-widths into the learning of a probability distribution. Specifically, for a given set of candidate bit-widths, $\mathbb{B} = \{b_1, b_2, \dots, b_m\}$, we aim to learn a probability distribution $\mathbf{p} = \{p_1, p_2, \dots, p_m\}$ for each feature group, where p_i denotes the likelihood of selecting b_i as the bit-width. To ensure the probabilities sum to 1, we maintain a learnable vector $\gamma = \{\gamma_1, \gamma_2, \dots, \gamma_m\}$ for each group and calculate the probabilities using the softmax function, as shown below:

$$p_i = \frac{e^{\gamma_i/\tau}}{\sum_{j=1}^m e^{\gamma_j/\tau}}, \quad (8)$$

where τ is the temperature used to control the optimization of γ , and a smaller τ brings \mathbf{p} closer to a one-hot distribution. Initially, all γ values are set to zero, ensuring that each candidate bit-width has an equal probability when training begins. When necessary, superscript k will be used for \mathbf{p} and γ to indicate their association with the k -th group.

Using the probability distribution above, each feature in a group has a specific probability of being quantized at various bit-widths. Therefore, we use the expected outcomes of quantizing the feature embedding at different bit-widths as the final quantized embedding, as shown in Figure 2. Specifically, for an embedding vector \mathbf{e} , the final quantized embedding $\bar{\mathbf{e}}$ will be computed as follows:

$$\bar{\mathbf{e}} = \sum_{i=1}^m p_i \times Q(\mathbf{e}, \alpha, \beta, b_i), \quad (9)$$

where Q is the base quantizer, LSQ+ [2], as discussed in Section 2.2. The quantized embedding $\bar{\mathbf{e}}$ is then fed into the subsequent

networks to compute the loss function. During backpropagation, the original embedding \mathbf{e} and the probability distribution parameter γ will be updated through gradient descent algorithms.

To balance the storage overhead of embedding tables with model prediction accuracy, we introduce regularization for the expected bit-width of each feature group. Given the correlation between feature importance and frequency, we utilize the sum of the feature frequencies within each group to adjust the regularization coefficients accordingly. Specifically, the objective function we optimize is defined as follows:

$$\mathcal{L} = \mathcal{L}_{CE} + \lambda \sum_{j=1}^g \frac{1}{s_j} \sum_{i=1}^m b_i \times p_i^j \quad (10)$$

where \mathcal{L}_{CE} represents the cross-entropy loss calculated between the model outputs and the ground-truth labels, s_j is the sum of feature frequencies in the j -th group, and λ is the regularization coefficient used to balance model accuracy and memory usage.

Additionally, we emphasize that maintaining separate step size and offset for each feature is both memory-intensive and unnecessary. Instead, quantization with different bit-widths necessitates distinct step sizes, while varying dimensions of the embedding table require different offsets. Therefore, we adopt a single step size for each bit-width and a single offset for each embedding dimension.

3.4 Precision Sampling and Retraining

Through the optimization process illustrated in Figure 2, we can derive the probability distribution over candidate bit-widths, allowing us to determine each group's final bit-width. However, the bit-width with the highest probability may not necessarily be the most appropriate choice. Specifically, while a higher bit-width may not correspond to the highest probability, it can still contribute a considerable portion of high-precision representation to the final embedding. In this context, this feature group should be recognized as one that necessitates a higher bit-width. To this end, we select the highest bit-width with a probability exceeding the threshold of $\frac{1}{2m}$ as the final precision for each group, as outlined below:

$$b^* = \max\{b_i \mid p_i > \frac{1}{2m}, i \in [1, 2, \dots, m]\}, \quad (11)$$

where b^* is the sampled precision of a feature group. Bit-widths with a probability less than $\frac{1}{2m}$ are considered to have minimal contribution to the high-precision representation of embeddings.

On the other hand, directly quantizing the embedding parameters using the sampled bit-width may create discrepancies between the quantized embedding and that generated during training, thus affecting the model’s accuracy. This discrepancy arises because the embedding used during training result from combining quantization outcomes across all candidate bit-widths. To mitigate accuracy loss, we implement a retraining process using the sampled bit-widths to train mixed-precision embedding from scratch. Following the Lottery Ticket Hypothesis (LTH) [10], previous studies [31, 68] will reset the model parameters to the initialization values for retraining. However, to leverage the information from the search phase, we employ the optimized step size, offset, and feature interaction network to initialize the model in the retraining phase, aiming to enhance training outcomes. Note that only the embeddings are set back to the initialized values of the search phase during retraining.

4 IMPLEMENTATION

MPE is implemented as a plug-in embedding layer module based on PyTorch, which can be seamlessly integrated into existing recommendation models with minimal modifications. There are two stages in the implementation of MPE, training and inference. During training, embeddings are maintained as full-precision parameters, while during inference, they are supposed to be stored in low-precision formats. To enhance usability, the training and inference stages are encapsulated in separate modules.

During inference, MPE only requires storing embedding in mixed-precision formats and does not involve mixed-precision computations. Once the low-precision embeddings are retrieved, they must be dequantized into full-precision parameters before being fed into subsequent networks. Note that the input to the embedding table is highly sparse, and the embedding retrieved during forward propagation constitutes only a small proportion of the total. As a result, the storage overhead for dequantized embedding parameters is negligible. However, since frameworks such as PyTorch do not natively support data formats such as Int-2 and Int-3, we concatenate each embedding vector at the bit level and then divide them into the Int-16 format for storage. Upon feature retrieval, the corresponding Int-16 data will be converted into full-precision embedding.

5 EXPERIMENTS

In this section, we aim to demonstrate the superiority of MPE in embedding compression for DLRMs through extensive experiments, addressing the following research questions:

- **RQ1:** How does MPE compare to state-of-the-art methods in terms of compression efficiency for embedding tables?
- **RQ2:** How does retraining affect the performance of MPE?
- **RQ3:** Are the bit-widths optimized for a specific model applicable to other models?
- **RQ4:** How does MPE perform in terms of inference latency?
- **RQ5:** Is MPE capable of generating mixed-precision embeddings?

5.1 Experimental Settings

5.1.1 Datasets. The experiments are conducted on three real-world datasets: Avazu [46], Criteo [21], and KDD12 [1]. The Avazu dataset contains 10 days of click logs with 22 categorical feature fields. The Criteo dataset contains 7 days of ad click data with 26 categorical and 13 numerical feature fields. The KDD12 dataset has no temporal information and consists of 11 categorical feature fields. The statistics of the datasets are shown in Table 2.

Following previous work [27, 34], we preprocess the datasets as outlined below. For the Avazu dataset, we remove the instance_id field and transform the timestamp field into three new fields: hour, weekday, and is_weekend. For the Criteo dataset, each numeric value x is discretized into $\lfloor \log^2(x) \rfloor$ when $x > 2$; otherwise, x is set to 1. For all datasets, categorical features that appear only once are replaced with an “OOV” (out-of-vocabulary) token. Each dataset is then randomly split in the ratio of 8:1:1 to obtain the corresponding training, validation, and test sets.

Table 2: Statistics of the datasets.

Dataset	#Fields	#Features	#Samples	Positive Ratio
Avazu	22	9,449,445	40,428,967	16.98%
Criteo	39	33,762,577	45,840,617	25.62%
KDD12	11	54,689,798	149,639,105	4.45%

5.1.2 Models. In the experiments, we evaluated four widely-used models: DNN, DCN [51], DeepFM [15], and IPNN [42]. The DNN model employs a multi-layer perception (MLP) as the feature interaction network to process embeddings and generate predictions. In contrast, the other three models integrate additional modules for feature interaction modeling. In addition to the MLP, the DCN, DeepFM, and IPNN models integrate a cross network, a factorization machine (FM) [44], and an inner product layer, respectively. These four classic models represent different patterns of feature interaction and are chosen to demonstrate the versatility of MPE.

5.1.3 Baselines. We compare the proposed MPE with various embedding compression methods, including QR-Trick [45], ALPT [27], LSQ+ [2], PEP [31], OptFS [34]. QR-Trick is a hashing method, using multiple hash functions and complementary embedding tables to reduce the collisions among features. ALPT is an embedding quantization method, specifically a low-precision training method, which compresses both training and inference memory usage. LSQ+ is an advanced QAT method designed to quantize the weights and activations of convolutional neural networks with a specific bit-width. In this paper, we employ LSQ+ to compress embedding tables of DLRMs. PEP is to prune the feature embeddings with a learnable threshold. OptFS is a feature selection method that learns a gate scalar to decide whether to keep a feature. The implementations of all baselines strictly refer to the original papers or codes, which are available in the open source code repository.

5.1.4 Metrics. We assess the prediction accuracy of various methods on the test set using AUC (Area Under the ROC Curve) and Logloss (cross-entropy loss), where a higher AUC or lower Logloss indicates better recommendation performance. Note that a 0.001

Table 3: Performance comparison between MPE and baseline methods.

	Method	Avazu			Criteo			KDD12		
		AUC↑	Logloss↓	Ratio↓	AUC↑	Logloss↓	Ratio↓	AUC↑	Logloss↓	Ratio↓
DNN	Backbone	0.7955 ($\pm 1e-4$)	0.3704 ($\pm 1e-4$)	1.0000 ($\pm 0e+0$)	0.8106 ($\pm 2e-4$)	0.4413 ($\pm 2e-4$)	1.0000 ($\pm 0e+0$)	0.8219 ($\pm 2e-4$)	0.1473 ($\pm 1e-4$)	1.0000 ($\pm 0e+0$)
	QR-Trick	0.7899 ($\pm 2e-4$)	0.3741 ($\pm 1e-4$)	0.5000 ($\pm 0e+0$)	0.8078 ($\pm 1e-4$)	0.4437 ($\pm 1e-4$)	0.5000 ($\pm 0e+0$)	0.8088 ($\pm 2e-4$)	0.1502 ($\pm 1e-4$)	0.5000 ($\pm 0e+0$)
	PEP	0.7953 ($\pm 1e-4$)	0.3705 ($\pm 1e-4$)	0.9945 ($\pm 1e-5$)	0.8104 ($\pm 1e-4$)	0.4415 ($\pm 1e-4$)	0.0340 ($\pm 1e-3$)	0.8216 ($\pm 1e-4$)	0.1475 ($\pm 1e-4$)	0.9947 ($\pm 2e-4$)
	OptFS	0.7955 ($\pm 1e-4$)	0.3705 ($\pm 1e-4$)	0.9863 ($\pm 2e-4$)	0.8105 ($\pm 1e-4$)	0.4414 ($\pm 1e-4$)	0.0187 ($\pm 2e-4$)	0.8214 ($\pm 1e-4$)	0.1475 ($\pm 1e-4$)	0.9839 ($\pm 1e-4$)
	ALPT	0.7952 ($\pm 1e-4$)	0.3707 ($\pm 1e-4$)	0.2500 ($\pm 0e+0$)	0.8104 ($\pm 1e-4$)	0.4413 ($\pm 1e-4$)	0.2500 ($\pm 0e+0$)	0.8214 ($\pm 1e-4$)	0.1474 ($\pm 1e-4$)	0.2500 ($\pm 0e+0$)
	LSQ+	0.7954 ($\pm 1e-4$)	0.3705 ($\pm 1e-4$)	0.1875 ($\pm 0e+0$)	0.8104 ($\pm 1e-4$)	0.4414 ($\pm 1e-4$)	0.1875 ($\pm 0e+0$)	0.8220 ($\pm 1e-4$)	0.1473 ($\pm 0e+0$)	0.1875 ($\pm 0e+0$)
DCN	MPE	0.7959 ($\pm 5e-4$)	0.3702 ($\pm 3e-4$)	0.0573 ($\pm 7e-3$)	0.8104 ($\pm 1e-4$)	0.4415 ($\pm 1e-4$)	0.0055 ($\pm 4e-4$)	0.8218 ($\pm 3e-4$)	0.1475 ($\pm 5e-4$)	0.0409 ($\pm 3e-3$)
	Backbone	0.7956 ($\pm 2e-4$)	0.3703 ($\pm 1e-4$)	1.0000 ($\pm 0e+0$)	0.8106 ($\pm 2e-4$)	0.4413 ($\pm 2e-4$)	1.0000 ($\pm 0e+0$)	0.8224 ($\pm 2e-4$)	0.1472 ($\pm 1e-4$)	1.0000 ($\pm 0e+0$)
	QR-Trick	0.7901 ($\pm 1e-4$)	0.3740 ($\pm 1e-4$)	0.5000 ($\pm 0e+0$)	0.8078 ($\pm 1e-4$)	0.4437 ($\pm 1e-4$)	0.5000 ($\pm 0e+0$)	0.8094 ($\pm 1e-4$)	0.1502 ($\pm 2e-5$)	0.5000 ($\pm 0e+0$)
	PEP	0.7954 ($\pm 1e-4$)	0.3705 ($\pm 1e-4$)	0.9946 ($\pm 1e-5$)	0.8104 ($\pm 1e-4$)	0.4414 ($\pm 1e-4$)	0.0332 ($\pm 5e-4$)	0.8221 ($\pm 1e-4$)	0.1475 ($\pm 1e-4$)	0.9948 ($\pm 1e-4$)
	OptFS	0.7954 ($\pm 1e-4$)	0.3705 ($\pm 1e-4$)	0.9870 ($\pm 1e-5$)	0.8105 ($\pm 1e-4$)	0.4413 ($\pm 1e-4$)	0.0182 ($\pm 1e-4$)	0.8218 ($\pm 1e-4$)	0.1475 ($\pm 1e-4$)	0.9842 ($\pm 2e-4$)
	ALPT	0.7954 ($\pm 1e-4$)	0.3705 ($\pm 1e-4$)	0.2500 ($\pm 0e+0$)	0.8104 ($\pm 1e-4$)	0.4414 ($\pm 1e-4$)	0.2500 ($\pm 0e+0$)	0.8215 ($\pm 1e-4$)	0.1476 ($\pm 3e-5$)	0.2500 ($\pm 0e+0$)
DeepFM	LSQ+	0.7954 ($\pm 2e-4$)	0.3704 ($\pm 1e-4$)	0.1875 ($\pm 0e+0$)	0.8105 ($\pm 1e-4$)	0.4415 ($\pm 1e-4$)	0.1875 ($\pm 0e+0$)	0.8224 ($\pm 1e-4$)	0.1472 ($\pm 1e-4$)	0.1875 ($\pm 0e+0$)
	MPE	0.7956 ($\pm 3e-4$)	0.3703 ($\pm 2e-4$)	0.0551 ($\pm 7e-3$)	0.8105 ($\pm 1e-4$)	0.4414 ($\pm 1e-4$)	0.0051 ($\pm 5e-4$)	0.8224 ($\pm 3e-4$)	0.1471 ($\pm 3e-4$)	0.0496 ($\pm 3e-3$)
	Backbone	0.7956 ($\pm 1e-4$)	0.3704 ($\pm 1e-4$)	1.0000 ($\pm 0e+0$)	0.8100 ($\pm 1e-4$)	0.4419 ($\pm 1e-4$)	1.0000 ($\pm 0e+0$)	0.8219 ($\pm 3e-4$)	0.1474 ($\pm 1e-4$)	1.0000 ($\pm 0e+0$)
	QR-Trick	0.7899 ($\pm 1e-4$)	0.3741 ($\pm 4e-5$)	0.5000 ($\pm 0e+0$)	0.8068 ($\pm 2e-4$)	0.4446 ($\pm 2e-4$)	0.5000 ($\pm 0e+0$)	0.8080 ($\pm 2e-4$)	0.1504 ($\pm 1e-4$)	0.5000 ($\pm 0e+0$)
	PEP	0.7953 ($\pm 1e-4$)	0.3705 ($\pm 3e-5$)	0.9945 ($\pm 1e-4$)	0.8098 ($\pm 4e-5$)	0.4421 ($\pm 1e-4$)	0.0267 ($\pm 7e-4$)	0.8218 ($\pm 1e-4$)	0.1474 ($\pm 1e-4$)	0.9942 ($\pm 1e-4$)
	OptFS	0.7954 ($\pm 1e-4$)	0.3705 ($\pm 1e-4$)	0.9865 ($\pm 2e-4$)	0.8075 ($\pm 2e-4$)	0.4440 ($\pm 2e-4$)	0.0184 ($\pm 1e-4$)	0.8213 ($\pm 2e-4$)	0.1476 ($\pm 1e-4$)	0.9838 ($\pm 2e-4$)
IPNN	ALPT	0.7951 ($\pm 1e-4$)	0.3708 ($\pm 1e-4$)	0.2500 ($\pm 0e+0$)	0.8097 ($\pm 3e-5$)	0.4420 ($\pm 1e-4$)	0.2500 ($\pm 0e+0$)	0.8209 ($\pm 1e-4$)	0.1477 ($\pm 1e-4$)	0.2500 ($\pm 0e+0$)
	LSQ+	0.7955 ($\pm 1e-4$)	0.3704 ($\pm 3e-5$)	0.1875 ($\pm 0e+0$)	0.8099 ($\pm 1e-4$)	0.4419 ($\pm 1e-4$)	0.1875 ($\pm 0e+0$)	0.8218 ($\pm 1e-4$)	0.1474 ($\pm 1e-4$)	0.1875 ($\pm 0e+0$)
	MPE	0.7956 ($\pm 4e-4$)	0.3702 ($\pm 2e-4$)	0.0573 ($\pm 6e-3$)	0.8099 ($\pm 1e-4$)	0.4419 ($\pm 1e-4$)	0.0052 ($\pm 3e-4$)	0.8223 ($\pm 3e-4$)	0.1472 ($\pm 1e-4$)	0.0496 ($\pm 2e-3$)
	Backbone	0.7959 ($\pm 1e-4$)	0.3702 ($\pm 1e-4$)	1.0000 ($\pm 0e+0$)	0.8110 ($\pm 2e-4$)	0.4409 ($\pm 2e-4$)	1.0000 ($\pm 0e+0$)	0.8221 ($\pm 2e-4$)	0.1473 ($\pm 4e-5$)	1.0000 ($\pm 0e+0$)
	QR-Trick	0.7901 ($\pm 2e-4$)	0.3740 ($\pm 2e-4$)	0.5000 ($\pm 0e+0$)	0.8079 ($\pm 4e-5$)	0.4436 ($\pm 3e-5$)	0.5000 ($\pm 0e+0$)	0.8083 ($\pm 2e-4$)	0.1503 ($\pm 1e-4$)	0.5000 ($\pm 0e+0$)
	PEP	0.7956 ($\pm 1e-4$)	0.3704 ($\pm 1e-4$)	0.9945 ($\pm 3e-5$)	0.8104 ($\pm 2e-5$)	0.4414 ($\pm 2e-5$)	0.0451 ($\pm 2e-4$)	0.8218 ($\pm 3e-4$)	0.1474 ($\pm 1e-4$)	0.9946 ($\pm 2e-4$)
IPNN	OptFS	0.7956 ($\pm 1e-4$)	0.3704 ($\pm 1e-4$)	0.9869 ($\pm 1e-4$)	0.8108 ($\pm 4e-5$)	0.4411 ($\pm 4e-5$)	0.0188 ($\pm 1e-4$)	0.8216 ($\pm 5e-5$)	0.1475 ($\pm 3e-5$)	0.9844 ($\pm 1e-4$)
	ALPT	0.7957 ($\pm 2e-4$)	0.3705 ($\pm 1e-4$)	0.2500 ($\pm 0e+0$)	0.8108 ($\pm 1e-4$)	0.4410 ($\pm 1e-4$)	0.2500 ($\pm 0e+0$)	0.8213 ($\pm 1e-4$)	0.1475 ($\pm 5e-5$)	0.2500 ($\pm 0e+0$)
	LSQ+	0.7957 ($\pm 1e-4$)	0.3703 ($\pm 1e-4$)	0.1875 ($\pm 0e+0$)	0.8109 ($\pm 1e-4$)	0.4409 ($\pm 5e-5$)	0.1875 ($\pm 0e+0$)	0.8221 ($\pm 2e-4$)	0.1473 ($\pm 5e-5$)	0.1875 ($\pm 0e+0$)
	MPE	0.7960 ($\pm 2e-4$)	0.3700 ($\pm 3e-4$)	0.0609 ($\pm 7e-3$)	0.8108 ($\pm 1e-4$)	0.4412 ($\pm 1e-4$)	0.0053 ($\pm 3e-4$)	0.8220 ($\pm 3e-4$)	0.1473 ($\pm 1e-4$)	0.0412 ($\pm 1e-3$)

increase in AUC is generally considered a significant improvement. To assess compression efficiency, we present the embedding storage ratios relative to uncompressed embedding tables across different methods. Additionally, we discuss inference latency in Section 5.5.

5.1.5 Hyperparameters. We set various hyperparameters following previous work to ensure that our backbone has sufficiently excellent performance. Specifically, we set the embedding dimension to 16 and initialize the embedding parameters by a normal distribution with a standard deviation of 3e-3. For all four models, we use a three-layer MLP where the size of the fully-connect layers are 1024, 512, 256, respectively. Adam [24] is employed as the optimizer. The batch size is set to 10000 and Batch Normalization [19] is used to ensure stable training. The learning rate is carefully tuned among {1e-4, 3e-4, 1e-3, 3e-3, 1e-2} and the weight decay is tuned among {0.0, 1e-7, 3e-7, 1e-6, 3e-6, 1e-5}. It turns out that the optimal learning rate is 1e-3, the optimal weight decay coefficient of the Avazu and KDD12 datasets is 0.0, and that of the Criteo dataset is 3e-6. Additionally, both the Avazu and KDD12 datasets reached optimal accuracy at the end of the first epoch, and overfitting occurred immediately after entering the second epoch. Therefore, we train one epoch on the Avazu and KDD12 datasets while training 8 epochs on the Criteo dataset. For MPE, we set the temperature coefficient τ to 3e-3 and the group size to 128. These two parameters require little tuning. The set of candidate bit-widths is set to {0, 1, 2, 3, 4, 5, 6}, where the maximum bit width is determined by the performance of LSQ+. Specifically, LSQ+ achieves a minimum bit-width of 6 without sacrificing prediction accuracy on all three datasets. We mainly adjust the regularization coefficient λ among {1e-6, 3e-6,

1e-5, 3e-5, 1e-4, 3e-4} for MPE to achieve a trade-off between model accuracy and compression ratio. For more detailed implementation, please refer to the open-source code. Each experiment is run at least five times on Nvidia 3090 GPUs with Intel Xeon E5-2673 CPUs. Average results and the standard deviation are reported.

5.2 Overall Performance (RQ1)

In this section, we primarily address two questions: (1) the maximum compression strength of various methods without losing accuracy, and (2) how the accuracy of these methods varies with different compression ratios. Specifically, we regulate the compression ratio for each method by adjusting relevant hyper-parameters, such as the bit-width for LSQ+ and ALPT. However, the QR-trick achieves a minimum compression ratio of 2x and cannot provide lossless compression, making it an exception.

Table 3 presents the accuracy and compression ratios of various methods at lossless compression, which demonstrates that the compression efficiency of MPE significantly surpasses that of other baselines. Specifically, MPE achieves approximately 18, 200, and 20 times compression on embedding tables without comprising prediction accuracy on the three datasets, where the average bit widths are 1.8, 0.16, and 1.6, respectively. The QR-trick shares embeddings across features, which diminishes feature discrimination when multiple features use the same representation. Even with just a 2x compression, the QR-trick leads to significant accuracy loss. LSQ+ achieves a minimum bit-width of 6 without compromising accuracy on all three datasets. Due to the lack of full-precision parameter support during training, ALPT requires a minimum bit-width of 8, which is slightly higher than that of LSQ+. From the

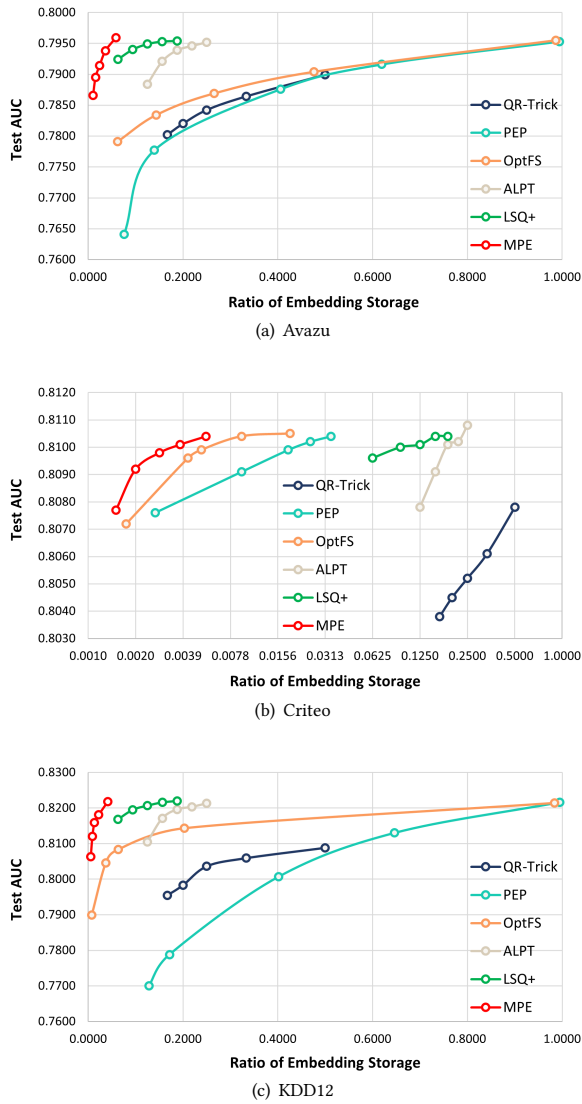


Figure 3: AUC under varying compression ratios.

pruning perspective, PEP and OptFS prune the embedding table at the element-level and row-level, respectively. They have some compression under the Criteo dataset, while the compression under the Avazu and KDD12 datasets is almost negligible, suggesting that there are few useless features or redundant parameters under the latter two datasets. However, LSQ+ can still compress embeddings into 6-bit integer parameters under the Avazu and KDD12 datasets, which indicates that the redundancy in the bit-width of parameters is significantly higher than that in the number of parameters. In contrast, on the Criteo dataset, the compression performance of LSQ+ is inferior to OptFS and PEP, primarily due to the uniform bit-width applied by LSQ+. Even when some features could be represented with fewer bits, they must use the same bit-width as more important features. Compared to LSQ+, MPE achieves finer-grained

compression through the proposed mixed-precision mechanism, assigning different bit-widths to different features. Compared to OptFS and PEP, MPE can also distinguish the importance of different features and achieves more efficient compression by reducing the precision of embedding parameters. Figure 3 illustrates the accuracy of various methods across different compression ratios, employing the DNN model. Obviously, at the same compression ratio, MPE consistently outperforms all baseline methods in terms of the AUC.

5.3 Ablation on Retraining (RQ2)

In this section, we examine the impact of retraining on MPE. We evaluated two variants: one without retraining and another with retraining using the LTH, where all parameters are reset to their initial values from the search phase. As shown in Table 4, quantizing embeddings with the sampled bit-widths without retraining leads to a significant loss of accuracy. However, retraining with LTH can partially mitigate this loss, although some degradation in accuracy remains. In MPE, we use the best-performing parameters, except for embeddings, to improve the initialization of the retrained model, resulting in substantial gains in accuracy. Moreover, the impact of retraining varies across datasets, with minimal effects on the Criteo dataset and more significant effects on the other two datasets.

Table 4: Ablation on retraining with the DNN model.

retraining	Avazu		Criteo		KDD12	
	AUC	LogLoss	AUC	LogLoss	AUC	LogLoss
w.o.	0.7919	0.3728	0.8102	0.4415	0.8190	0.1483
LTH	0.7930	0.3722	0.8105	0.4413	0.8204	0.1477
MPE	0.7959	0.3702	0.8104	0.4415	0.8218	0.1475

5.4 Transferability (RQ3)

In this section, we analyze the transferability of MPE, which specifically refers to the performance of applying the sampled bit-widths from a specific model to other models for retraining. It is important to note that MPE utilizes the step size, offset, and feature interaction network from the search phase to initialize the model during retraining. However, the structure of feature interaction networks may differ across models. Thus, we only reuse overlapping parameters. The models involved in the search and retraining processes are referred to as the source and target models, respectively.

Figure 4 presents the test AUC of the target model using various source models. To evaluate transferability, comparisons should be made within each column, ensuring that the target model remains consistent. On the Criteo dataset, sampled bit-widths can be transferred between different model architectures without impacting retraining accuracy. This aligns with the results in Table 4, which indicate that retraining has little impact on the Criteo dataset. In contrast, for the Avazu and KDD12 datasets, transferring search results across architectures occasionally reduces model accuracy. This implies that feature precision under these datasets is more sensitive to the structure of the feature interaction network. Moreover, the reduction in accuracy can be partially attributed to the inability to fully reuse the parameters of the feature interaction network generated during the search phase. However, compared to the

		Target Model			
		DNN	DCN	DeepFM	IPNN
Source Model	DNN	0.7959	0.7959	0.7956	0.7954
	DCN	0.7955	0.7956	0.7957	0.7956
	DeepFM	0.7952	0.7953	0.7956	0.7955
	IPNN	0.7948	0.7942	0.7949	0.7960

		Target Model			
		DNN	DCN	DeepFM	IPNN
Source Model	DNN	0.8104	0.8106	0.8096	0.8106
	DCN	0.8106	0.8105	0.8098	0.8108
	DeepFM	0.8107	0.8106	0.8099	0.8107
	IPNN	0.8104	0.8105	0.8098	0.8108

		Target Model			
		DNN	DCN	DeepFM	IPNN
Source Model	DNN	0.8218	0.8217	0.8217	0.8219
	DCN	0.8217	0.8224	0.8214	0.8218
	DeepFM	0.8217	0.8217	0.8223	0.8211
	IPNN	0.8222	0.8225	0.8226	0.8220

Figure 4: Transferability analysis. Each column contains the test AUC of a specific target model with different source models.

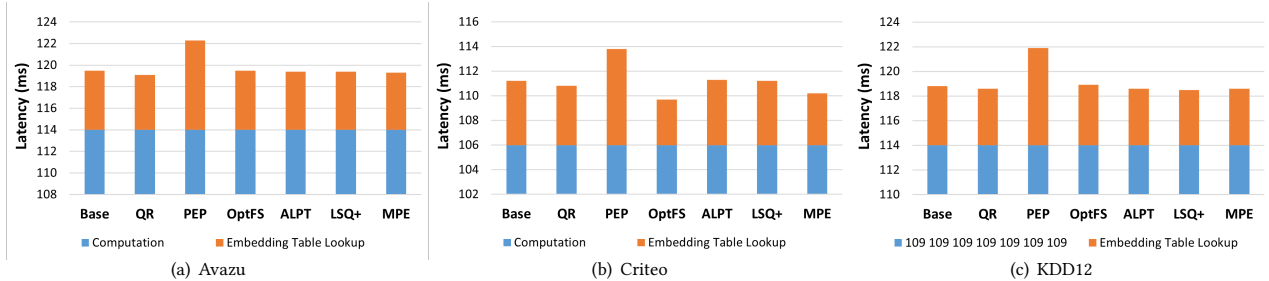


Figure 5: Inference latency of the DNN model using different compression methods.

accuracy loss observed without retraining, the loss incurred from transferring search results between different models is negligible.

5.5 Inference Latency (RQ4)

In this section, we evaluate the inference latency of different methods using the DNN model. The batch size used for inference is 10000. The primary difference among the methods lies in the embedding layer, and the time consumed by subsequent computations remain consistent. Therefore, we represent the inference latency as two parts: embedding table lookup and computation. As illustrated in Figure 5, the time spent on table lookup is significantly shorter than that on data loading and computation, resulting in no substantial difference in overall inference latency across methods. Notably, PEP requires sparse matrix storage for embedding compression, which adds latency to the table lookup process. OptFS reduces the number of features, especially for the Criteo dataset, thereby accelerating table lookup. Methods such as ALPT, LSQ+, and MPE reduce the storage overhead of embedding vectors, speeding up table lookup. However, the dequantization process of low-precision data slightly offsets the acceleration effect.

5.6 Bit-width Adjustment Capability (RQ5)

In this section, we provide a detailed examination of the sampled bit-widths. The candidate bit-widths of MPE range from $\{0, 1, 2, 3, 4, 5, 6\}$. Assigning a bit-width of 0 to a feature produces a zero vector for the corresponding embedding, which is equivalent to performing feature selection. As shown in Figure 6, the Avazu and

KDD12 datasets exhibit minimal redundancy in features, whereas the Criteo dataset displays a greater degree of redundancy, consistent with the experimental results of OptFS. Additionally, Figure 6 demonstrates that MPE can dynamically adjust bit-widths across different feature groups. The sampled bit-widths further indicate a positive correlation between feature precision and frequency.

6 RELATED WORK

6.1 Embedding Compression

Numerous studies have explored embedding compression techniques in recommendation models. Li et al. [28] provide a comprehensive survey of these methods, classifying them into three categories: low-precision, mixed-dimension, and weight-sharing, which target parameter, vector, and matrix-level compression, respectively. Our proposed method search for an ideal precision for each feature embedding, falling under the low-precision category.

Low-precision methods aim to reduce the precision of embedding parameters through quantization techniques. However, as discussed in Section 1, embedding quantization has received relatively less attention, with most research focusing on low-precision training (LPT) due to its effectiveness in memory compression during training [27, 58, 61]. **Mixed-dimension methods** aim to reduce the size of embedding vectors. For example, CpRec [47] assigns smaller embedding dimensions to less frequent features, while MDE [11] adjusts the embedding dimensions according to the size of the

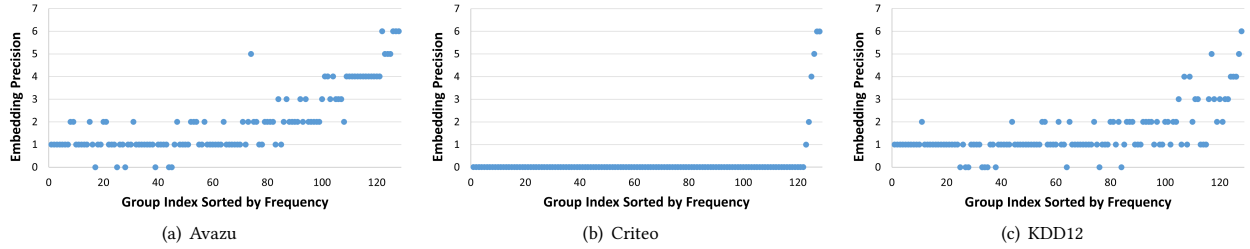


Figure 6: Embedding precision of different feature groups.

associated feature fields. Recent research has utilized neural architecture search (NAS) techniques [69] to search feature dimensions. For example, ESAPN [30] maintains a policy network optimized via reinforcement learning algorithms to decide when to increase embedding dimensions. Further, AutoEmb [67] designs dimension search algorithm through differential architecture search (DARTS) techniques [29]. Additionally, embedding pruning is essentially a mixed-dimension method. PEP [31] prunes embedding vectors by learning a threshold that dynamically determines the embedding size for different features. **Weight-sharing methods** aim to reduce the number of parameters actually used by embedding tables. For example, DoubleHash [64] allows less frequent features to share embeddings. ROBE applies more advanced hash functions to map each embedding parameter into a shared memory space, enhancing compression efficiency. On the other hand, Wu et al. [55] employs vector quantization to capture the similarity among features. They first cluster the most frequent embeddings to generate a codebook composed of several codewords. Then, each feature embedding is approximately represented by its most similar codeword. Note that vector quantization is essentially the clustering of vectors, which differs from the parameter quantization discussed in this paper.

6.2 Mixed-Precision Quantization

In mixed-precision neural networks, prior research has primarily focused on assigning different precision levels across layers to reduce memory consumption and computational overhead [7, 43, 50, 54, 62]. They can be categorized into three categories: gradient-based, heuristic-based, and reinforcement learning-based methods. **Gradient-based methods** usually convert the discrete precision selection problem into a continuous one, facilitating optimization through gradient descent algorithms. Wu et al. [54] propose a differentiable neural architecture search (DNAS) strategy, which utilizes Gumbel Softmax [20] to achieve differentiable precision selection. Subsequent studies, such as BP-NAS [63], GMPQ [53], and SEAM [49], have improved upon DNAS. **Heuristic-based methods** develop reasonable sensitivity metrics to assign precision. For example, HAWQ [7, 62] uses Hessian information to guide precision assignment, while Hybrid-Net [4] applies principal component analysis (PCA) to identify significant layers and assign higher precision accordingly. **Reinforcement learning-based methods**, like HAQ [50] and ADRL [40], employ reinforcement learning algorithms to search for optimal precision levels. In this paper, we reformulate the precision search as a precision probability distribution learning

problem, where the distribution is updated directly via gradient descent, making it a gradient-based method.

On the other hand, most mixed precision training methods consist of two stages: search and retraining [7, 54, 62]. The search stage identifies the optimal precision configuration, while the retraining stage usually fine-tunes the model to improve accuracy. However, some studies directly apply mixed-precision quantization to pre-trained models [3, 5] or train a mixed-precision network from scratch without retraining [48]. MPE requires retraining, and the exploration of retraining-free mixed-precision embeddings is left for future work.

7 CONCLUSION

In this paper, we identify a critical drawback of quantization-aware training for embedding compression, that is its inability to distinguish feature importance. To this end, we propose the mixed-precision embeddings (MPE) algorithm to enhance the compression efficiency, which identifies an appropriate precision for each feature to balance model accuracy and memory usage. Specifically, we first group features by frequency to simplify the search space for precision and then learn a probability distribution over precision levels for each group. MPE will sample the final bit-widths based on the optimized probability distribution and then retrain the model to achieve better accuracy. Extensive experiments are conducted to evaluate the performance of MPE. The results demonstrate that the MPE significantly outperforms the state-of-the-art methods, achieving a 200-fold compression without any loss in prediction accuracy on the Criteo dataset. Additionally, MPE is implemented as a plug-in embedding layer module based on PyTorch, ensuring ease of use.

REFERENCES

[1] Yi Wang Aden. 2012. KDD Cup 2012, Track 2. <https://kaggle.com/competitions/kddcup2012-track2>

[2] Yash Bhagat, Jinwon Lee, Markus Nagel, Tijmen Blankevoort, and Nojun Kwak. 2020. LSQ+: Improving low-bit quantization through learnable offsets and better initialization. In *2020 IEEE/CVF Conference on Computer Vision and Pattern Recognition, CVPR Workshops 2020.*, Computer Vision Foundation / IEEE, Seattle, WA, USA, 2978–2985.

[3] Yaohui Cai, Zhewei Yao, Zhen Dong, Amir Gholami, Michael W. Mahoney, and Kurt Keutzer. 2020. ZeroQ: A Novel Zero Shot Quantization Framework. In *2020 IEEE/CVF Conference on Computer Vision and Pattern Recognition, CVPR 2020*. Computer Vision Foundation / IEEE, Seattle, WA, USA, 13166–13175.

[4] Indranil Chakraborty, Deboleena Roy, Isha Garg, Aayush Ankit, and Kaushik Roy. 2020. Constructing energy-efficient mixed-precision neural networks through principal component analysis for edge intelligence. *Nat. Mach. Intell.* 2, 1 (2020), 43–55.

[5] Arun Chauhan, Utsav Tiwari, and Vikram N. R. 2023. Post Training Mixed Precision Quantization of Neural Networks using First-Order Information. In *IEEE/CVF International Conference on Computer Vision, ICCV 2023 - Workshops*. IEEE, Paris, France, 1335–1344.

[6] Wei Deng, Junwei Pan, Tian Zhou, Deguang Kong, Aaron Flores, and Guang Lin. 2021. DeepLight: Deep Lightweight Feature Interactions for Accelerating CTR Predictions in Ad Serving. In *WSDM '21, The Fourteenth ACM International Conference on Web Search and Data Mining*. ACM, Virtual Event, Israel, 922–930.

[7] Zhen Dong, Zhewei Yao, Amir Gholami, Michael W. Mahoney, and Kurt Keutzer. 2019. HAWQ: Hessian AWare Quantization of Neural Networks with Mixed-Precision. In *2019 IEEE/CVF International Conference on Computer Vision, ICCV 2019*. IEEE, Seoul, Korea (South), 293–302.

[8] Abhimanyu Dubey, Abhinav Jauhri, Abhinav Pandey, and et al. 2024. The Llama 3 Hurd of Models. *CoRR* abs/2407.21783 (2024).

[9] Steven K. Esser, Jeffrey L. McKinstry, Deepika Bablani, Rathinakumar Appuswamy, and Dharmendra S. Modha. 2020. Learned Step Size quantization. In *8th International Conference on Learning Representations, ICLR 2020*. OpenReview.net, Addis Ababa, Ethiopia.

[10] Jonathan Frankle and Michael Carbin. 2019. The Lottery Ticket Hypothesis: Finding Sparse, Trainable Neural Networks. In *7th International Conference on Learning Representations, ICLR*. OpenReview.net, New Orleans, LA, USA.

[11] Antonio A. Ginart, Maxim Naumov, Dheevatsa Mudigere, Jiyang Yang, and James Zou. 2021. Mixed Dimension Embeddings with Application to Memory-Efficient Recommendation Systems. In *IEEE International Symposium on Information Theory, ISIT 2021*. IEEE, Melbourne, Australia, 2786–2791.

[12] Aditya Grover and Jure Leskovec. 2016. node2vec: Scalable Feature Learning for Networks. In *Proceedings of the 22nd ACM SIGKDD International Conference on Knowledge Discovery and Data Mining*. ACM, San Francisco, CA, USA, 855–864.

[13] Hui Guan, Andrey Malevich, Jiyang Yang, Jongssoo Park, and Hector Yuen. 2019. Post-Training 4-bit Quantization on Embedding Tables. *CoRR* abs/1911.02079 (2019).

[14] Michael Günther. 2018. FREDDY: Fast Word Embeddings in Database Systems. In *Proceedings of the 2018 International Conference on Management of Data, SIGMOD Conference 2018*. ACM, Houston, TX, USA, 1817–1819.

[15] Huifeng Guo, Ruiming Tang, Yuning Ye, Zhenguo Li, and Xiuqiang He. 2017. DeepFM: A Factorization-Machine based Neural Network for CTR Prediction. In *26th International Joint Conference on Artificial Intelligence, IJCAI 2017. ijcai.org*, Melbourne, Australia, 1725–1731.

[16] Yi Guo, Zhaocheng Liu, Jianchao Tan, Chao Liao, Daqing Chang, Qiang Liu, Sen Yang, Ji Liu, Dongying Kong, Zhi Chen, and Chengru Song. 2022. LPFS: Learnable Polarizing Feature Selection for Click-Through Rate Prediction. *CoRR* abs/2206.00267 (2022).

[17] Geoffrey Hinton. 2012. Neural networks for machine learning. *Coursera video lectures* (2012).

[18] Lu Hou, Jinhua Zhu, James T. Kwok, Fei Gao, Tao Qin, and Tie-Yan Liu. 2019. Normalization Helps Training of Quantized LSTM. In *Advances in Neural Information Processing Systems 32: Annual Conference on Neural Information Processing Systems 2019, NeurIPS 2019*. Curran Associates, Vancouver, BC, Canada, 7344–7354.

[19] Sergey Ioffe and Christian Szegedy. 2015. Batch Normalization: Accelerating Deep Network Training by Reducing Internal Covariate Shift. In *Proceedings of the 32nd International Conference on Machine Learning, ICML 2015*. JMLR.org, Lille, France, 448–456.

[20] Eric Jang, Shixiang Gu, and Ben Poole. 2017. Categorical Reparameterization with Gumbel-Softmax. In *5th International Conference on Learning Representations, ICLR 2017*. OpenReview.net, Toulon, France.

[21] Olivier Chapelle Jean-Baptiste Tien, joycenv. 2014. Display Advertising Challenge. <https://kaggle.com/competitions/criteo-display-ad-challenge>

[22] Pengyue Jia, Yeqing Wang, Zhaocheng Du, Xiangyu Zhao, Yichao Wang, Bo Chen, Wanyu Wang, Huifeng Guo, and Ruiming Tang. 2024. ERASE: Benchmarking Feature Selection Methods for Deep Recommender Systems. In *Proceedings of the 30th ACM SIGKDD Conference on Knowledge Discovery and Data Mining, KDD 2024*, Ricardo Baeza-Yates and Francesco Bonchi (Eds.). ACM, Barcelona, Spain, 5194–5205.

[23] Wang-Cheng Kang, Derek Zhiyuan Cheng, Ting Chen, Xinyang Yi, Dong Lin, Lichan Hong, and Ed H. Chi. 2020. Learning Multi-granular Quantized Embeddings for Large-Vocab Categorical Features in Recommender Systems. In *Companion of The 2020 Web Conference 2020*. ACM / IW3C2, Taipei, Taiwan, 562–566.

[24] Diederik P. Kingma and Jimmy Ba. 2015. Adam: A Method for Stochastic Optimization. In *3rd International Conference on Learning Representations, ICLR 2015*. OpenReview.net, San Diego, CA, USA.

[25] Fan Lai, Wei Zhang, Rui Liu, William Tsai, Xiaohan Wei, Yuxi Hu, Sabin Devkota, Jianyu Huang, Jongssoo Park, Xing Liu, Zeliang Chen, Ellie Wen, Paul Rivera, Jie You, Chun-cheng Jason Chen, and Mosharaf Chowdhury. 2023. AdaEmbed: Adaptive Embedding for Large-Scale Recommendation Models. In *17th USENIX Symposium on Operating Systems Design and Implementation, OSDI 2023*. USENIX Association, Boston, MA, USA, 817–831.

[26] Rui Li, Chaozhuo Li, Yanming Shen, Zeyu Zhang, and Xu Chen. 2024. Generalizing Knowledge Graph Embedding with Universal Orthogonal Parameterization. In *Forty-first International Conference on Machine Learning, ICML 2024*. OpenReview.net, Vienna, Austria.

[27] Shiwei Li, Hufeng Guo, Lu Hou, Wei Zhang, Xing Tang, Ruiming Tang, Rui Zhang, and Ruixuan Li. 2023. Adaptive Low-Precision Training for Embeddings in Click-Through Rate Prediction. In *Thirty-Seventh AAAI Conference on Artificial Intelligence, AAAI 2023*. AAAI Press, Washington, DC, USA, 4435–4443.

[28] Shiwei Li, Hufeng Guo, Xing Tang, Ruiming Tang, Lu Hou, Ruixuan Li, and Rui Zhang. 2024. Embedding Compression in Recommender Systems: A Survey. *ACM Comput. Surv.* 56, 5 (2024), 130:1–130:21.

[29] Hanxiao Liu, Karen Simonyan, and Yiming Yang. 2019. DARTS: Differentiable Architecture Search. In *7th International Conference on Learning Representations, ICLR 2019*. OpenReview.net, New Orleans, LA, USA.

[30] Haochen Liu, Xiangyu Zhao, Chong Wang, Xiaobing Liu, and Jiliang Tang. 2020. Automated Embedding Size Search in Deep Recommender Systems. In *Proceedings of the 43rd International ACM SIGIR conference on research and development in Information Retrieval, SIGIR 2020*. ACM, Virtual Event, China, 2307–2316.

[31] Siyi Liu, Chen Gao, Yihong Chen, Depeng Jin, and Yong Li. 2021. Learnable Embedding sizes for Recommender Systems. In *9th International Conference on Learning Representations, ICLR 2021*. OpenReview.net, Virtual Event, Austria.

[32] Yuval Lev Lubarsky, Jan Tönshoff, Martin Grohe, and Benny Kimelfeld. 2023. Selecting Walk Schemes for Database Embedding. In *Proceedings of the 32nd ACM International Conference on Information and Knowledge Management, CIKM 2023*. ACM, Birmingham, United Kingdom, 1677–1686.

[33] Fuyuan Lyu, Xing Tang, Hufeng Guo, Ruiming Tang, Xiuqiang He, Rui Zhang, and Xue Liu. 2022. Memorize, Factorize, or be Naive: Learning Optimal Feature Interaction Methods for CTR Prediction. In *38th IEEE International Conference on Data Engineering, ICDE 2022*. IEEE, Kuala Lumpur, Malaysia, 1450–1462.

[34] Fuyuan Lyu, Xing Tang, Dugang Liu, Liang Chen, Xiuqiang He, and Xue Liu. 2023. Optimizing Feature Set for Click-Through Rate Prediction. In *Proceedings of the ACM Web Conference 2023, WWW 2023*. ACM, Austin, TX, USA, 3386–3395.

[35] Fuyuan Lyu, Xing Tang, Hong Zhu, Hufeng Guo, Yingxue Zhang, Ruiming Tang, and Xue Liu. 2022. OptEmbed: Learning Optimal Embedding Table for Click-through Rate Prediction. In *Proceedings of the 31st ACM International Conference on Information & Knowledge Management*. ACM, Atlanta, GA, USA, 1399–1409.

[36] Tomás Mikolov, Kai Chen, Greg Corrado, and Jeffrey Dean. 2013. Efficient Estimation of Word Representations in Vector Space. In *1st International Conference on Learning Representations, ICLR 2013, Workshop Track Proceedings*. OpenReview.net, Scottsdale, Arizona, USA.

[37] Markus Nagel, Rana Ali Amjad, Mart van Baalen, Christos Louizos, and Tijmen Blankevoort. 2020. Up or Down? Adaptive Rounding for Post-Training Quantization. In *Proceedings of the 37th International Conference on Machine Learning, ICML 2020 (Proceedings of Machine Learning Research)*, Vol. 119. PMLR, Virtual Event, 7197–7206.

[38] Markus Nagel, Marios Fournarakis, Rana Ali Amjad, Yelysei Bondarenko, Mart van Baalen, and Tijmen Blankevoort. 2021. A White Paper on Neural Network Quantization. *CoRR* abs/2106.08295 (2021).

[39] Markus Nagel, Marios Fournarakis, Yelysei Bondarenko, and Tijmen Blankevoort. 2022. Overcoming Oscillations in Quantization-Aware Training. In *International Conference on Machine Learning, ICML 2022 (Proceedings of Machine Learning Research)*, Vol. 162. PMLR, Baltimore, Maryland, USA, 16318–16330.

[40] Lin Ning, Guoyang Chen, Weifeng Zhang, and Xipeng Shen. 2021. Simple Augmentation Goes a Long Way: ADRL for DNN Quantization. In *9th International Conference on Learning Representations, ICLR 2021*. OpenReview.net, Virtual Event, Austria.

[41] Rajvardhan Patil, Sorio Boit, Venkat N. Gudiyada, and Jagadeesh Nandigam. 2023. A Survey of Text Representation and Embedding Techniques in NLP. *IEEE Access* 11 (2023), 36120–36146.

[42] Yanru Qu, Han Cai, Kan Ren, Weinan Zhang, Yong Yu, Ying Wen, and Jun Wang. 2016. Product-Based Neural Networks for User Response Prediction. In *IEEE 16th*

International Conference on Data Mining, ICDM 2016. IEEE Computer Society, Barcelona, Spain, 1149–1154.

[43] Mariam Rakka, Mohammed E. Fouda, Pramod Khargonekar, and Fadi J. Kurdahi. 2022. Mixed-Precision Neural Networks: A Survey. *CoRR* abs/2208.06064 (2022).

[44] Steffen Rendle. 2010. Factorization Machines. In *ICDM 2010, The 10th IEEE International Conference on Data Mining, Sydney, Australia, 14-17 December 2010.* IEEE Computer Society, Sydney, Australia, 995–1000.

[45] Hao-Jun Michael Shi, Dheevatsa Mudigere, Maxim Naumov, and Jiyan Yang. 2020. Compositional Embeddings Using Complementary Partitions for Memory-Efficient Recommendation Systems. In *KDD '20: The 26th ACM SIGKDD Conference on Knowledge Discovery and Data Mining.* ACM, Virtual Event, CA, USA, 165–175.

[46] Will Cukierski Steve Wang. 2014. Click-Through Rate Prediction. <https://kaggle.com/competitions/avazu-ctr-prediction>

[47] Yang Sun, Fajie Yuan, Min Yang, Guoao Wei, Zhou Zhao, and Duo Liu. 2020. A Generic Network Compression Framework for Sequential Recommender Systems. In *Proceedings of the 43rd International ACM SIGIR conference on research and development in Information Retrieval, SIGIR 2020.* ACM, Virtual Event, China, 1299–1308.

[48] Chen Tang, Yuan Meng, Jiacheng Jiang, Shuzhao Xie, Rongwei Lu, Xinzhua Ma, Zhi Wang, and Wenwu Zhu. 2024. Retraining-free Model Quantization via One-Shot Weight-Coupling Learning. *CoRR* abs/2401.01543 (2024).

[49] Chen Tang, Kai Ouyang, Zenghao Chai, Yunpeng Bai, Yuan Meng, Zhi Wang, and Wenwu Zhu. 2023. SEAM: Searching Transferable Mixed-Precision Quantization Policy through Large Margin Regularization. In *Proceedings of the 31st ACM International Conference on Multimedia, MM 2023.* ACM, Ottawa, ON, Canada, 7971–7980.

[50] Kuan Wang, Zhijian Liu, Yujun Lin, Ji Lin, and Song Han. 2019. HAQ: Hardware-Aware Automated Quantization With Mixed Precision. In *IEEE Conference on Computer Vision and Pattern Recognition, CVPR 2019.* Computer Vision Foundation / IEEE, Long Beach, CA, USA, 8612–8620.

[51] Ruoxi Wang, Bin Fu, Gang Fu, and Mingliang Wang. 2017. Deep & Cross Network for Ad Click Predictions. In *Proceedings of the ADKDD'17.* ACM, Canada, 12:1–12:7.

[52] Ruoxi Wang, Rakesh Shivanna, Derek Zhiyuan Cheng, Sagar Jain, Dong Lin, Lichan Hong, and Ed H. Chi. 2021. DCN V2: Improved Deep & Cross Network and Practical Lessons for Web-scale Learning to Rank Systems. In *WWW '21: The Web Conference 2021.* ACM / IW3C2, Virtual Event / Ljubljana, Slovenia, 1785–1797.

[53] Ziwei Wang, Han Xiao, Jiwen Lu, and Jie Zhou. 2021. Generalizable Mixed-Precision Quantization via Attribution Rank Preservation. In *2021 IEEE/CVF International Conference on Computer Vision, ICCV 2021.* IEEE, Montreal, QC, Canada, 5271–5280.

[54] Bichen Wu, Yanghan Wang, Peizhao Zhang, Yuandong Tian, Peter Vajda, and Kurt Keutzer. 2018. Mixed Precision Quantization of ConvNets via Differentiable Neural Architecture Search. *CoRR* abs/1812.00090 (2018).

[55] Xiaorui Wu, Hong Xu, Honglin Zhang, Huaming Chen, and Jian Wang. 2020. Saec: similarity-aware embedding compression in recommendation systems. In *APSys '20: 11th ACM SIGOPS Asia-Pacific Workshop on Systems.* ACM, Tsukuba, Japan, 82–89.

[56] Jun Xiao, Hao Ye, Xiangnan He, Hanwang Zhang, Fei Wu, and Tat-Seng Chua. 2017. Attentional Factorization Machines: Learning the Weight of Feature Interactions via Attention Networks. In *Proceedings of the Twenty-Sixth International Joint Conference on Artificial Intelligence, IJCAI 2017.* ijcai.org, Melbourne, Australia, 3119–3125.

[57] Tesi Xiao, Xia Xiao, Ming Chen, and Youlong Chen. 2022. Field-wise Embedding Size Search via Structural Hard Auxiliary Mask Pruning for Click-Through Rate Prediction. In *Proceedings of the Workshop on Deep Learning for Search and Recommendation (DL4SR 2022) co-located with the 31st ACM International Conference on Information and Knowledge Management (CIKM 2022) (CEUR Workshop Proceedings).* Wei Liu and Linsey Pang (Eds.), Vol. 3317. CEUR-WS.org, Atlanta, Georgia, USA.

[58] Zhiqiang Xu, Dong Li, Weijie Zhao, Xing Shen, Tianbo Huang, Xiaoyun Li, and Ping Li. 2021. Agile and Accurate CTR Prediction Model Training for Massive-Scale Online Advertising Systems. In *SIGMOD '21: International Conference on Management of Data.* ACM, Virtual Event, China, 2404–2409.

[59] Bencheng Yan, Pengjie Wang, Jinquan Liu, Wei Lin, Kuang-Chih Lee, Jian Xu, and Bo Zheng. 2021. Binary Code based Hash Embedding for Web-scale Applications. In *CIKM '21: The 30th ACM International Conference on Information and Knowledge Management.* ACM, Virtual Event, Queensland, Australia, 3563–3567.

[60] Enneng Yang, Xin Xin, Li Shen, Yudong Luo, and Guibing Guo. 2024. Generalized Embedding Machines for Recommender Systems. *Mach. Intell. Res.* 21, 3 (2024), 571–584.

[61] Jie Amy Yang, Jianyu Huang, Jongsoo Park, Ping Tak Peter Tang, and Andrew Tulloch. 2020. Mixed-Precision Embedding Using a Cache. *CoRR* abs/2010.11305 (2020).

[62] Zhewei Yao, Zhen Dong, Zhangcheng Zheng, Amir Gholami, Jiali Yu, Eric Tan, Leyuan Wang, Qijing Huang, Yida Wang, Michael W. Mahoney, and Kurt Keutzer. 2021. HAWQ-V3: Dyadic Neural Network Quantization. In *Proceedings of the 38th International Conference on Machine Learning, ICML 2021 (Proceedings of Machine Learning Research),* Vol. 139. PMLR, Virtual Event, 11875–11886.

[63] Haibao Yu, Qi Han, Jianbo Li, Jianping Shi, Guangliang Cheng, and Bin Fan. 2020. Search What You Want: Barrier Panely NAS for Mixed Precision Quantization. In *Computer Vision - ECCV 2020 - 16th European Conference, Proceedings, Part IX (Lecture Notes in Computer Science),* Vol. 12354. Springer, Glasgow, UK, 1–16.

[64] Caojin Zhang, Yicun Liu, Yuanyu Xie, Sofia Ira Ktena, Alykhan Tejani, Akshay Gupta, Pranay Kumar Myana, Deepak Dilipkumar Suvadip Paul, Ikuhiro Ihara, Prasang Upadhyaya, Ferenc Huszar, and Wenzhe Shi. 2020. Model Size Reduction Using Frequency Based Double Hashing for Recommender Systems. In *RecSys 2020: Fourteenth ACM Conference on Recommender Systems.* ACM, Virtual Event, Brazil, 521–526.

[65] Hailin Zhang, Zirui Liu, Boxuan Chen, Yikai Zhao, Tong Zhao, Tong Yang, and Bin Cui. 2024. CAFE: Towards Compact, Adaptive, and Fast Embedding for Large-scale Recommendation Models. *Proc. ACM Manag. Data* 2, 1 (2024), 51:1–51:28.

[66] Weinan Zhang, Jiarui Qin, Wei Guo, Ruiming Tang, and Xiuqiang He. 2021. Deep Learning for Click-Through Rate Estimation. In *Proceedings of the Thirtieth International Joint Conference on Artificial Intelligence, IJCAI 2021.* ijcai.org, Virtual Event / Montreal, Canada, 4695–4703.

[67] Xiangyu Zhao, Haochen Liu, Wenqi Fan, Hui Liu, Jiliang Tang, Chong Wang, Ming Chen, Xudong Zheng, Xiaobing Liu, and Xiwang Yang. 2021. AutoEmb: Automated Embedding Dimensionality Search in Streaming Recommendations. (2021), 896–905.

[68] Xiangyu Zhao, Haochen Liu, Hui Liu, Jiliang Tang, Weiwei Guo, Jun Shi, Sida Wang, Huiji Gao, and Bo Long. 2021. AutoDim: Field-aware Embedding Dimension Searchin Recommender Systems. In *WWW '21: The Web Conference 2021.* ACM / IW3C2, Virtual Event, Ljubljana, Slovenia, 3015–3022.

[69] Barret Zoph and Quoc V. Le. 2017. Neural Architecture Search with Reinforcement Learning. In *5th International Conference on Learning Representations, ICLR 2017.* OpenReview.net, Toulon, France.